



1 **Investigation on the feasibility of straw incorporation to improve soil 2 fertility without obviously increasing global warming potential**

3 Mengxue Zhang^{1, 2}, Rujia Liao^{1, 2}, Wenzhao Zhang¹, Cheng Fang¹, Simon Guerrero-Cruz³, András
4 Táncsics⁴, Baoli Zhu¹, Wenxue Wei¹, Rong Sheng¹

5 ¹Taoyuan Station of Agro-Ecology Research, Institute of Subtropical Agriculture, Chinese Academy of Sciences, Changsha
6 410125, China

7 ²College of Resource and Environment, University of Chinese Academy of Sciences, Beijing 100049, China

8 ³Department of Water Resources and Environmental Engineering, Asian Institute of Technology, Pathum Thani 12120,
9 Thailand

10 ⁴Hungarian University of Agriculture and Life Sciences, Páter K. u. 1., H-2100, Gödöllő, Hungary

11 *Correspondence to:* Rong Sheng (shengrong@isa.ac.cn)

12 **Abstract.** The utility of rice straw as an organic fertilizer has been widely recognized as a promising approach to enhancing
13 soil fertility. However, straw return is currently in a dilemma, as it may also provoke greenhouse gas (GHG) emissions,
14 leading to serious environmental consequences. It is urgent to reveal the feasibility of straw incorporation regarding soil
15 fertility improvement without notable increases in GHG emissions. Here, a soil microcosm experiment was employed to
16 investigate the relationships between soil fertility and GHG fluxes and the underlying mechanisms influenced by straw
17 amendments. Paddy soils were collected from a long-term rice straw incorporation field experiment. The dynamics of GHG
18 fluxes and concentrations in soils, and the variations in the abundances of soil microbial communities were systematically
19 determined. The results indicated that continuous rice straw incorporation at half of the harvest (ST1) obviously improved
20 soil fertility but did not induce significant elevation of global warming potential (GWP). The minimal increase in GWP was
21 mainly attributed to the significant reduction in N₂O emission and the slight rise in CH₄ emission compared to straw removal.
22 The main mechanisms for these consequences were that ST1 possessed the highest *nosZII* abundance and the lowest
23 *nirS/nosZII* ratio; meanwhile, its CH₄ production ability fluctuated around the soil CH₄ holding capacity, and most of the
24 produced CH₄ was consumed by methanotrophs. In conclusion, rice straw can be incorporated into paddy soils at a suitable
25 application rate, which can effectively enhance soil fertility without inducing an additional warming effect.

26 **1 Introduction**

27 Rice cultivation not only provides staple food for nearly half of the global population, but also produces massive rice straw
28 that is estimated to be 800 to 1000 million tons·year⁻¹ globally (Yuan et al., 2021; Harun et al., 2022). Rice straw has long
29 been a valuable organic resource that can be incorporated into rice paddies to improve soil productivity (Huo et al., 2024;
30 Zhou et al., 2024). The incorporation can enhance soil carbon (C) sequestration (Chen et al., 2025; Li et al., 2025a). It was
31 estimated that about 15%–25% of the incorporated straw C was converted into soil organic carbon (SOC) (Liu et al., 2023b).



32 Straw return can also provide abundant available nutrients for rice plant growth, including nitrogen (N), phosphorus (P), and
33 potassium (K) (Yin et al., 2018; Van Hung et al., 2020; Wang et al., 2020). Thus, rice straw incorporation has been proposed
34 to be an important agronomic practice for sustainable rice agriculture.

35 However, rice straw return was also revealed to exacerbate greenhouse gas (GHG) emissions from paddy fields (Shi et al.,
36 2023; He et al., 2024). Rice cultivation contributes around 12% of global agricultural GHG emissions (Fao, 2020) with straw
37 incorporation being one of the key drivers. Numerous studies indicated that compared to straw removal, rice straw
38 incorporation substantially promoted methane (CH_4) emissions (Han et al., 2023; Song et al., 2024; Qin et al., 2025). The
39 increases in CH_4 emissions varied widely across observations, which approximately ranged from 23% to 1192% (Shen et al.,
40 2014; Jiang et al., 2019; Lee et al., 2020; Nan et al., 2022; Song et al., 2024). The incorporation may also elevate carbon
41 dioxide (CO_2) fluxes from rice paddies, for example, by 9% to 67% (Shen et al., 2014; Lee et al., 2020; Han et al., 2023;
42 Song et al., 2024). However, the effect of rice straw incorporation on nitrous oxide (N_2O) emissions from rice fields was
43 inconsistent and controversial across studies (Shen et al., 2014; Wang et al., 2015; Han et al., 2023; Qin et al., 2023). The
44 variations in N_2O emissions were about -73% to 137% in comparison with their controls (Shen et al., 2014; Wang et al.,
45 2015; Han et al., 2023; Qin et al., 2023). Despite these issues, managing the straw input rate was suggested to mitigating the
46 straw-induced GHG emissions (Shen et al., 2014; Chen et al., 2018; Li et al., 2024). For instance, incorporating with half of
47 the harvested rice straw effectively reduced CH_4 emission by 48% in relative to the scenario receiving full of the straw (Shen
48 et al., 2014). However, most studies focused either on the influence of straw return on soil productivity (Huo et al., 2024;
49 Zhou et al., 2024) or on GHG emissions (Shi et al., 2023; He et al., 2024), rarely taking both into consideration to reveal the
50 rational straw application. Hence, it is essential to investigate the feasibility of straw incorporation not causing noticeable
51 increases in GHG emissions while improving soil fertility.

52 Here, a soil culture experiment was employed to continue the field experiment with 5-year rice straw incorporation at
53 different rates. The incubation was set with flooding and drying periods. The dynamics of GHG emissions and
54 concentrations in soils were determined, and the variations in the abundance of soil microbial communities involved in GHG
55 production and consumption were measured. This study aimed to explore whether there is a suitable straw application rate
56 that can boost soil fertility without causing elevated GHG emissions, and the related mechanisms.

57 2 Materials and methods

58 2.1 Soil collection and rice straw preparation

59 Soils were collected from a long-term straw return field experiment initiated in 2017, which was located at the Taoyuan
60 Agroecosystem Research Station (28°55' N, 111°26' E), Hunan, China. The region has a subtropical monsoon climate with a
61 mean annual rainfall of 1440 mm and a mean annual temperature of 16.5°C. The soil was derived from quaternary red clay
62 and classified as Ultisol according to USDA soil taxonomy. The experiment contained various rates of rice straw
63 amendments with three replications in a randomized block design. Each plot was 30 m² (7.5 m × 4 m) and the cropping was



64 single rice. Rice straw was evenly spread on the surface of the corresponding plots and turned over into the soils in each
65 early May, which was about one month ahead of rice seedling transplantation. Besides, urea, superphosphate, and potassium
66 chloride were annually applied to all treatments at $112.60 \text{ kg N}\cdot\text{ha}^{-1}$, $46.33 \text{ kg P}\cdot\text{ha}^{-1}$, and $135.46 \text{ kg K}\cdot\text{ha}^{-1}$, respectively.

67 The soils (0–20 cm) were separately taken from CK, ST1, ST2, and ST3 treatments of the field experiment in May 2022
68 before straw application. The corresponding straw amounts were 0, 3750, 7500, and $11250 \text{ kg}\cdot\text{ha}^{-1}$, representing 0, 50%,
69 100%, and 150% of the local rice straw yield, respectively. The soil from one treatment was collected by taking five points
70 following an “S” pattern in each plot and mixed, and then transported to the lab. After removal of visible plant residues and
71 gravel, the soils were pre-incubated under flooding in a greenhouse for 30 days. The soil physicochemical properties were
72 shown in Table 1.

73 Rice straw was prepared by collecting it from the field in October 2021, followed by air-drying and grinding (< 1 mm) for
74 the microcosm experiment. The rice straw contained 44.14% of C, 0.817% of N, 2.34% of K, and 0.143% of P.

75 2.2 Microcosm experiment

76 The incubation pots were prepared by sealing the bottoms of PVC cylinders (height 15 cm, diameter 15.5 cm). The pots for
77 gas sampling were further equipped as follows (Fig.S1). For soil gas sampling, two holes (diameter 1.7 cm) across the
78 cylinder were drilled at positions of 5 cm from the bottom, filled with a gas-permeable silicone tube (length 15.5 cm, inner
79 diameter 1.2 cm) closed at both ends with silicone septa. One end was connected with a three-way stopcock outside the
80 cylinder via a stainless steel tube (diameter 0.2 cm) through the septum. The drilled holes in the cylinder wall were then
81 sealed. For gas flux sampling, a hollow rectangular groove (deep 2 cm) was fixed on the top fringe of each pot for water
82 sealing during sampling. The gas sampling was carried out using a static chamber (height 29.5 cm, diameter 19.5 cm) fitted
83 with a small electric fan at the inner top.

84 The pre-incubated soil slurries from different treatments were separately filled into the pots, and each pot contained 1.27 kg
85 (dry weight) of soil to reach about 10 cm in depth. The incubation followed the field regime and the straw amendment rates
86 were calculated based on the field experiment, which were 0, 2.54, 5.08, and 7.62 g rice straw per pot for CK, ST1, ST2, and
87 ST3 treatments, respectively. Each treatment had eight pots: three for gas sampling, three for soil sampling, and two for
88 replacing sampling-induced soil cylinders to minimize gas exchange from the sampled holes.

89 After urea ($100 \text{ mg N}\cdot\text{kg}^{-1}$ dry soil) and straw were applied, the soil was mixed thoroughly, and deionized water was added
90 to meet a 3 cm water layer. Then, the microcosms were randomly positioned and incubated in the dark at 30°C for 91 days
91 (28-day flooding and 63-day drying). This incubation period was based on our pre-experiment to cover both CH_4 and N_2O
92 emission peaks. During the flooding, a 3 cm top water layer was maintained with deionized water. The drying process was
93 carried out by removing the top water from the microcosm with a syringe on day 28 and then drying by natural evaporation
94 in the room.



95 2.3 Gas and soil sampling

96 Gas samples for both GHG fluxes and soil concentrations were taken at 1–3 day(s) intervals. At each sampling event, after
97 the groove was filled with water and covered by the chamber, 30 mL headspace gas was taken with a syringe at 0 and 60 min
98 separately from each gas sampling pot (Wang et al., 2017; Zhou et al., 2020). The electric fan was running during the
99 sampling period. At the same time, 1 mL soil gas was taken from the buried silicone tube, followed by an equal volume of
100 helium injected back. All the gas samples were stored in 12 mL pre-evacuated extainer vials (Labco, UK).
101 Soil samples (0–5 cm) were taken every two weeks via a modified syringe sampler with its head cut off. At each sampling
102 event, three cores (diameter 1.5 cm) were sampled from each pot and mixed, weighing about 35 g wet soil. During flooding,
103 the soil samples were collected directly without removing the overlying water to minimize the disturbance (Cai et al., 2022;
104 Cai et al., 2025). Before starting soil sampling, placing the front end of the syringe sampler as close as possible to the soil
105 surface effectively reduced the collection of overlying water. A part of the sample was used for soil moisture measurement,
106 and the rest was flash-frozen in liquid nitrogen and stored at -80°C for molecular analysis. After sampling, the holes were
107 immediately replaced by filling with the cores taken from the soil replacement pots.

108 2.4 Analysis of gas concentrations and soil properties

109 Gas samples were analyzed using a gas chromatography (7890A, Agilent, USA) equipped with an electron capture detector
110 for N₂O and a flame ionization detector for CH₄ and CO₂. Gas fluxes were calculated based on the Ideal Gas Law (Eq. 1 and
111 Eq. 2), and cumulative emissions by the Trapezoidal Rule (Eq. 3). Global warming potential (GWP) was calculated using
112 cumulative emissions (Eq. 4).

$$113 F = \frac{\Delta m}{A \times \Delta t}, \quad (1)$$

114 Where F is the gas flux ($\mu\text{g} \cdot \text{m}^{-2} \cdot \text{h}^{-1}$); Δm is the mass of gas collected in a single sampling event (μg); A is the soil surface
115 area covered by the static chamber (m^{-2}); Δt is the time interval after chamber closure (h).

$$116 \Delta m = M \times \Delta n = M \times \frac{pV \times \Delta c}{RT}, \quad (2)$$

117 Where M is the molar mass of gas ($\text{g} \cdot \text{mol}^{-1}$); Δn is the amount of substance of gas collected in a single sampling event (mol);
118 p is the atmospheric pressure (Pa); V is the active volume of the static chamber during sampling (m^3); Δc is the gas
119 concentration difference (ppm); R is the gas constant ($8.314 \text{ J} \cdot \text{mol}^{-1} \cdot \text{K}^{-1}$); T is the temperature during sampling (K).

$$120 CE = \sum_{i=1}^n \frac{F_{i+1} + F_i}{1000} \times (t_{i+1} - t_i) \times 24 \times \frac{1}{2}, \quad (3)$$

121 Where CE is the gas cumulative emission ($\text{g} \cdot \text{m}^{-2}$); F is the gas flux ($\mu\text{g} \cdot \text{m}^{-2} \cdot \text{h}^{-1}$); 1000 in the denominator is to transform μg
122 to g; t is the sampling time (d); i and $i+1$ represent the i^{th} and $(i+1)^{\text{th}}$ sampling events, respectively; 24 is the transform factor
123 from day to hour; n is the total number of sampling events.

$$124 GWP = CE_{CO_2} + 27.9 \times CE_{CH_4} + 273 \times CE_{N_2O}, \quad (4)$$



125 Where the unit of GWP is g CO₂ equivalent·m⁻². CE_{CO_2} , CE_{CH_4} , and CE_{N_2O} represent the cumulative emissions (g·m⁻²) of
126 CO₂, CH₄, and N₂O, respectively. The factors 27.9 and 273 are the latest-updated 100-year global warming potentials for
127 CH₄ and N₂O, respectively (Forster et al., 2021).

128 Soil properties were measured by standard protocols (Bao, 2000). Soil pH was determined using soil slurry at a soil–water
129 ratio of 1:2.5 by a pH meter (FE28–Standard, Mettler Toledo, Switzerland). Soil bulk density (BD) was measured by the ring
130 knife method. Soil cation exchange capacity (CEC) was extracted by 1.66 cM Co(NH₃)₆Cl₃ at a soil–extractant ratio of 7:100.
131 Olsen P was extracted by 0.5 M NaHCO₃ at a soil–extractant ratio of 1:20. Soil CEC and Olsen P were quantified
132 colorimetrically via a continuous–flow automatic analyzer (AutoAnalyzer 3, SEAL Analytic, Germany). Available N (Av_N)
133 was determined by the alkaline diffusion method. Available K (Av_K) was extracted by 1 M NH₄OAc at a soil–extractant
134 ratio of 1:10 and analyzed via an atomic absorption spectrometer (novAA350, Analytic Jena, Germany). Soil available
135 manganese (Av_Mn), copper (Av_Cu), and zinc (Av_Zn) were simultaneously extracted by 5 mM DTPA–CaCl₂–TEA at a
136 soil–extractant ratio of 1:2 and determined by an inductively coupled plasma emission spectrometer (ICP–OES 5110,
137 Agilent, USA). Soil total C (TC) and total N (TN) were analyzed by combustion using an elemental analyzer (Vario MAX
138 cube, Elementar, Germany). Soil total P (TP) and total K (TK) were measured by the ICP–OES after digestion by HNO₃–
139 HClO₄–HF.

140 **2.5 DNA extraction and real-time quantitative PCR**

141 Soil DNA was extracted manually as previously described (Chen et al., 2010). Each sample was performed in triplicate. The
142 quality and concentration of DNA were measured by a NanoDrop ND–1000 spectrophotometer (Thermo Scientific, USA).
143 The abundances of bacterial 16S rRNA, fungal 18S rRNA, *mcrA*, *pmoA*, *nirS*, and *nosZII* were determined by real-time
144 quantitative PCR (qPCR). The genes of *mcrA* and *pmoA* were used as markers for methanogens and aerobic methanotrophs,
145 respectively (Liu et al., 2025). The genes of *nirS* and *nosZII* were selected to reflect N₂O production (Chen et al., 2024;
146 Kong et al., 2024) and N₂O reduction (Jones et al., 2013; Hallin et al., 2018; Liu et al., 2023a; Yang et al., 2024),
147 respectively. The qPCR primers and thermal programs were shown in Table S1. All qPCR reactions were conducted in
148 triplicate on 384-well plates by a LightCycler 480II (Roche, Switzerland). Each reaction (10 µL) contained 1 µL of template
149 DNA (5 ng·µL⁻¹), 5 µL of SYBR Green Pro Taq HS Premix (Accurate Biotechnology, China), and 0.3–1.2 µL of each
150 primer (10 µM). Negative controls were included in each plate by replacing the template DNA with sterile H₂O. Standard
151 curves were prepared by ten-fold serial dilutions of target gene-carrying plasmids. The amplification efficiency was 87%–88%
152 for *nosZII* and 90%–102% for other genes.

153 **2.6 Statistical analysis**

154 Statistical tests were performed in IBM SPSS Statistics 25 (NY, USA) and OriginPro 2026 (OriginLab Corporation, MA,
155 USA). Homoscedasticity ($\alpha = 0.05$) was checked with Levene's test. Significant differences between treatments ($\alpha = 0.05$)



156 were tested by one-way analysis of variance (ANOVA), followed by Tukey's Honestly Significant Difference (HSD) test
157 when data were homoscedastic or Games-Howell (GH) test when data were heteroscedastic.

158 3 Results

159 3.1 Soil properties

160 Soil physicochemical characteristics were clearly affected by continuous straw incorporation at various rates for five years
161 (Table 1). Although the concentrations of soil TP and TK were not strongly influenced by straw application, the
162 concentrations of TC, TN, available nutrients, and CEC were positively related to the straw incorporation rate and soil BD
163 was negatively related to the rate. When compared with CK, even in the treatment with the least amount of straw (ST1), the
164 TC and TN contents were increased by 4.19% and 2.58%, respectively. ST1 treatment also resulted in obvious increases in
165 Av_N, Olsen P, and Av_K by 6.83%, 15.09%, and 38.52% ($p < 0.05$), respectively. Furthermore, the contents of soil
166 available micronutrients of Mn, Cu, and Zn in ST1 treatment were also increased by 18.48%, 4.57%, and 8.09%,
167 respectively.

168 **Table 1: Soil properties after five-year straw incorporation at different rates**

	pH (H ₂ O) (1:2.5)	BD g·cm ⁻³	CEC cmol ⁺ ·kg ⁻¹	Av_N mg·kg ⁻¹	Olsen P mg·kg ⁻¹	Av_K mg·kg ⁻¹	Av_Mn mg·kg ⁻¹	Av_Cu mg·kg ⁻¹	Av_Zn mg·kg ⁻¹	TC g·kg ⁻¹	TN g·kg ⁻¹	TP g·kg ⁻¹	TK g·kg ⁻¹
CK	4.90± 0.03 a	1.45± 0.03 a	10.85± 0.15 a	192.79± 5.38 a	13.19± 1.76 a	51.09± 2.70 c	8.28± 0.22 a	1.75± 0.10 a	1.36± 0.07 a	21.74± 0.46 a	2.057± 0.04 a	0.618± 0.03 a	12.16± 0.08 a
ST1	4.98± 0.05 a	1.41± 0.01 a	11.19± 0.23 a	205.96± 3.59 a	15.18± 1.68 a	70.77± 3.62 bc	9.81± 1.50 a	1.83± 0.09 a	1.47± 0.10 a	22.65± 0.59 a	2.110± 0.05 a	0.657± 0.02 a	12.01± 0.11 a
ST2	4.93± 0.02 a	1.34± 0.07 a	11.25± 0.20 a	212.07± 8.15 a	12.57± 1.33 a	82.35± 5.01 ab	11.65± 2.30 a	1.94± 0.07 a	1.70± 0.07 a	23.52± 0.70 a	2.197± 0.07 a	0.610± 0.03 a	11.95± 0.19 a
ST3	5.02± 0.07 a	1.31± 0.03 a	11.45± 0.26 a	209.22± 11.70 a	16.06± 2.22 a	105.36± 11.01 a	16.69± 5.97 a	1.88± 0.05 a	1.76± 0.18 a	23.71± 1.45 a	2.160± 0.12 a	0.648± 0.04 a	12.04± 0.03 a

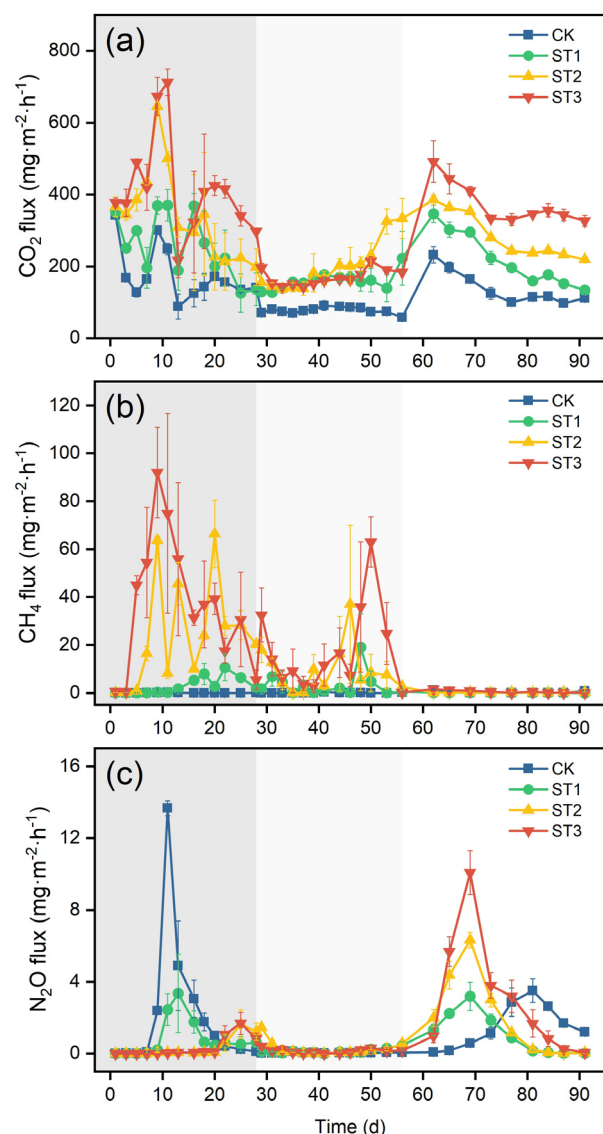
169 CK, ST1, ST2, and ST3 received 0, 50%, 100%, and 150% of the local harvested rice straw, respectively. Different lower-
170 case letters indicate significant differences between treatments ($\alpha = 0.05$). Data are given in average ± standard error (n = 3).
171 Abbreviations: BD, bulk density; CEC, cation exchange capacity; Av_N, available nitrogen; Olsen P, available phosphorus;
172 Av_K, available potassium; Av_Mn, available manganese; Av_Cu, available copper; Av_Zn, available zinc; TC, total
173 carbon; TN, total nitrogen; TP, total phosphorus; TK, total potassium.

174 3.2 CO₂, CH₄, and N₂O emissions

175 Greenhouse gas emissions were obviously influenced by straw incorporation (Fig.1). Generally, the CO₂ flux was positively
176 related to the straw incorporation rate throughout the incubation (Fig.1a). Compared to CK, ST1 caused a significant
177 increase in the cumulative CO₂ emission by 66% ($p < 0.05$, Table 2). With the straw amount increasing, the cumulative CO₂
178 emissions of ST2 and ST3 treatments rose to 2.2 and 2.5 times those of CK ($p < 0.05$), respectively. A significant difference
179 was also detected between ST2 and ST3 ($p < 0.05$).



180 The CH₄ fluxes occurred mainly during flooding (day 0–day 28), and partly during the transition time from flooding to
181 drying (day 29–day 56) (Fig.1b). It was observed that CK emitted minimal CH₄, while ST1 emitted a slightly higher CH₄
182 than CK. Further increasing the straw rate induced significant elevation of CH₄ fluxes. The more straw input, the more CH₄
183 was emitted. The cumulative CH₄ emission of ST1 was only 4.41 g·m⁻², while the cumulative CH₄ emissions of ST2 and
184 ST3 were approximately 4 and 8 times higher than those of ST1 ($p < 0.05$), respectively, reaching about 23 and 38 g·m⁻²
185 (Table 2).



186

187 **Figure 1: Dynamics of GHG fluxes during the incubation. (a) CO₂; (b) CH₄; (c) N₂O. Data are given in average ±**
188 **standard error (n = 3). Grey, lighter grey, and white areas indicate flooding, the early drained period, and the late**
189 **drained period, respectively.**



190 **Table 2: Cumulative emissions and global warming potential**

	Cumulative emissions			Global warming potential
	CO ₂ (g·m ⁻²)	CH ₄ (g·m ⁻²)	N ₂ O (g·m ⁻²)	(g CO ₂ equivalent·m ⁻²)
CK	280.19 ± 4.37 d	0.36 ± 0.02 d	2.61 ± 0.08 ab	1003.49 ± 24.74 c
ST1	465.65 ± 16.07 c	4.41 ± 0.52 c	1.63 ± 0.11 c	1034.95 ± 48.01 c
ST2	605.91 ± 26.84 b	23.22 ± 0.93 b	2.04 ± 0.17 bc	1810.05 ± 56.46 b
ST3	695.71 ± 17.59 a	38.01 ± 0.35 a	2.80 ± 0.20 a	2521.49 ± 80.01 a

191 Different lower-case letters indicate significant differences between treatments ($\alpha = 0.05$). Data are given in average ±
192 standard error (n = 3).

193 The dynamics of N₂O emission during the experiment exhibited two peaking periods: one occurred just after nitrogen
194 fertilization and the other happened during drying process, but the variation patterns of the flux peaks between the treatments
195 within the two peaking times were obviously different (Fig.1c). During the first peaking period, CK emitted most N₂O,
196 followed by ST1, while the N₂O emitted from ST2 and ST3 were negligible. However, this order reversed in the latter drying
197 period, where the highest N₂O flux was from ST3, followed by ST2, whereas the N₂O fluxes of ST1 and CK were similarly
198 low, despite that the peak of CK appeared about 10 days late. The cumulative N₂O emission indicated that ST1 emitted
199 significantly lower N₂O than CK ($p < 0.05$) with only 1.63 g·m⁻² (Table 2). Meanwhile, ST2 also generated about 22%
200 lower N₂O than CK, while the treatment receiving the highest amount of straw (ST3) possessed a similar cumulative N₂O
201 emission to CK.

202 Overall, ST1 displayed a slightly higher GWP than CK without a significant difference, but both ST2 and ST3 showed
203 significantly higher GWPs than CK ($p < 0.05$).

204 **3.3 Dynamics of CO₂, CH₄, and N₂O concentrations in soils**

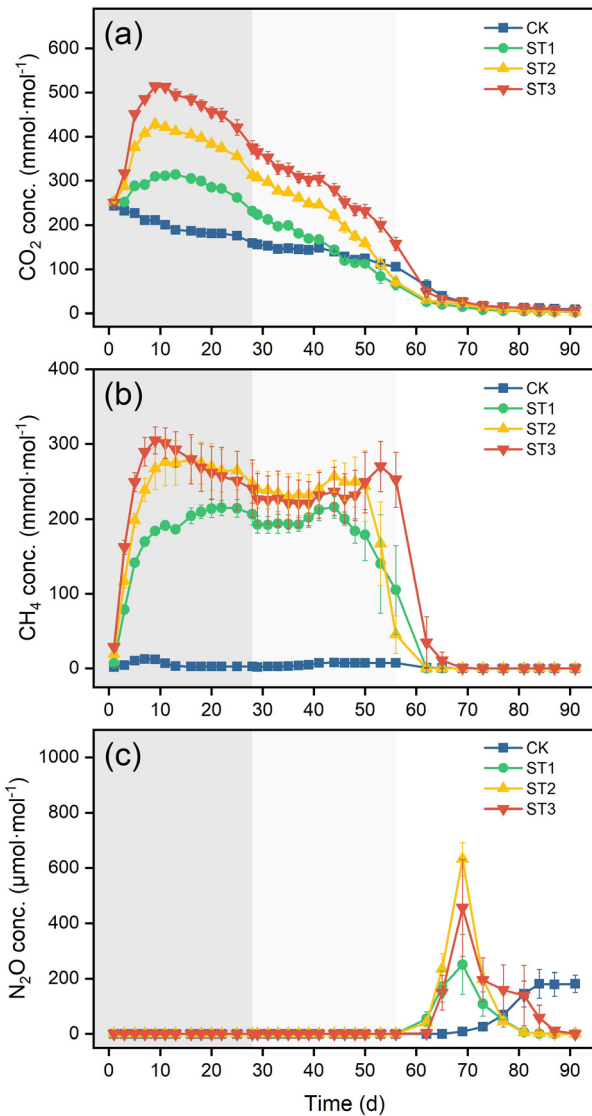
205 The soil concentrations of the three GHGs were deeply affected by the amendments of rice straw but exhibited distinct
206 patterns (Fig.2). Straw incorporation significantly increased soil CO₂ concentration compared to CK, with the peaking time
207 of straw-amended treatments occurring around 10 days of the incubation (Fig.2a). The outstanding characteristic of the
208 dynamics of CO₂ concentrations was that the increases were proportional to the straw incorporation rates. For example, at
209 the peaking time, the increments of ST1, ST2, and ST3 were approximately 50%, 100%, and 150% against CK, respectively.

210 The soil CH₄ concentrations indicated that straw incorporation resulted in sharp increases since day 3 (Fig.2b). On average,
211 the CH₄ concentrations of ST1, ST2, and ST3 were about 45, 57, and 58 times those of CK during day 1 and day 56. It was
212 also observed that the CH₄ concentrations of ST1 fluctuated around 200 mmol·mol⁻¹. The treatments of ST2 and ST3 further
213 promoted soil CH₄ concentrations but there was no significant difference between them.

214 The soil N₂O concentrations were only detectable between days 62 and 87 under drying phase (Fig.2c). The unique feature
215 was that the N₂O contents of CK and ST1 were quite similar despite the peaking time in CK was delayed. It was observed



216 that the N_2O concentration of ST2 was almost two times that of ST1. Although the peak of ST3 was not as high as that of
217 ST2, ST3 maintained high N_2O concentrations for longer in the soil.



218

219 **Figure 2: Dynamics of GHG concentrations in soils during the incubation. (a) CO_2 ; (b) CH_4 ; (c) N_2O . The abbreviation *conc.***
220 **means concentration. Data are given in average \pm standard error ($n = 3$).** Grey, lighter grey, and white areas indicate flooding, the
221 **early drained period, and the late drained period, respectively.**

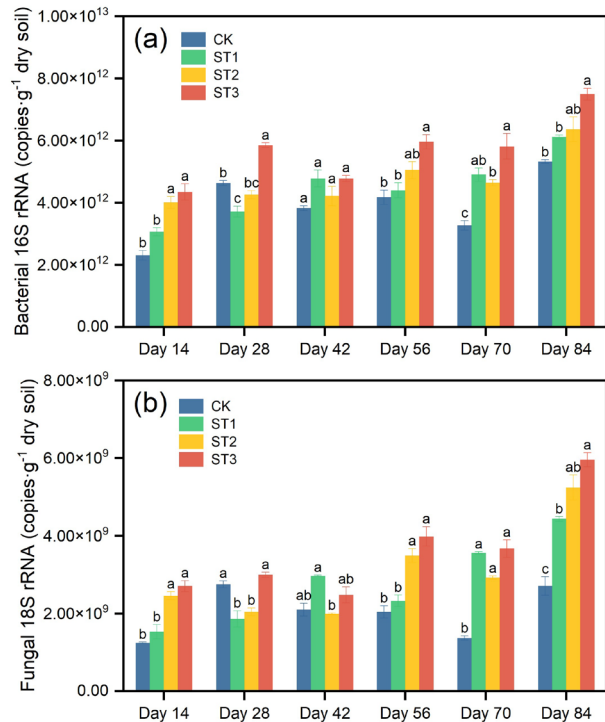
222 3.4 Variations of microbial abundance

223 3.4.1 The abundance of bacteria and fungi

224 In general, the abundance of both bacterial 16S rRNA and fungal 18S rRNA followed the order of ST3 > ST2 > ST1 > CK
225 (Fig.3). The average copy numbers of 16S rRNA were 3.92E+12, 4.50E+12, 4.76E+12, and 5.71E+12 per gram dry soil for



226 CK, ST1, ST2, and ST3, respectively. The average abundances of 18S rRNA were 2.04E+9, 2.78E+9, 3.03E+9, and 3.63E+9
227 per gram dry soil, respectively.



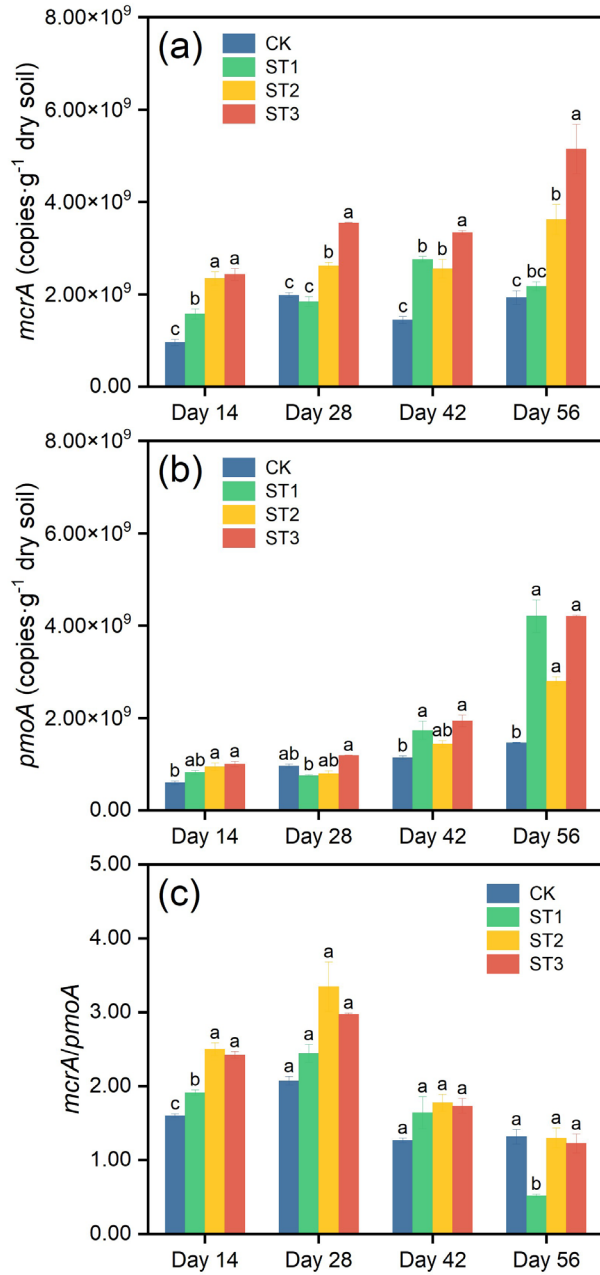
228
229 **Figure 3: Dynamics of bacterial 16S rRNA abundance (a) and fungal 18S rRNA abundance (b) during the incubation. Different**
230 **lower-case letters denote significant differences between treatments ($\alpha = 0.05$). Data are given in average \pm standard error (n = 3).**

231 3.4.2 The abundance of methanogens (*mcrA*) and methanotrophs (*pmoA*)

232 The copy number of *mcrA* was obviously affected by straw incorporation and positively related to the straw input rate
233 (Fig.4a). The average *mcrA* abundance during the CH₄ fluxing period between day 14 and day 56 was significantly and
234 positively related to the straw input rate. In comparison with CK, the least increase occurred in ST1 with 32%, while the
235 highest happened in ST3 with 129%.

236 For *pmoA*, although straw incorporation also clearly promoted its copy number, the treatment with the lowest amount of
237 straw (ST1) induced a substantial increase in methanotrophs compared to CK by approximately 81%. Further increasing the
238 straw amount failed to cause significant elevations in comparison with ST1 (Fig.4b).

239 When concerning *mcrA*/*pmoA*, the ratio of ST1 was quite similar to that of CK, while the ratios of ST2 and ST3 were
240 significantly higher than that of CK (Fig.4c).



241

242 **Figure 4: Dynamics of *mcrA* abundance (a), *pmoA* abundance (b), and *mcrA/pmoA* ratio (c) during the CH₄ fluxing**

243 period. Different lower-case letters denote significant differences between treatments ($\alpha = 0.05$). Data are given in

244 average \pm standard error ($n = 3$).

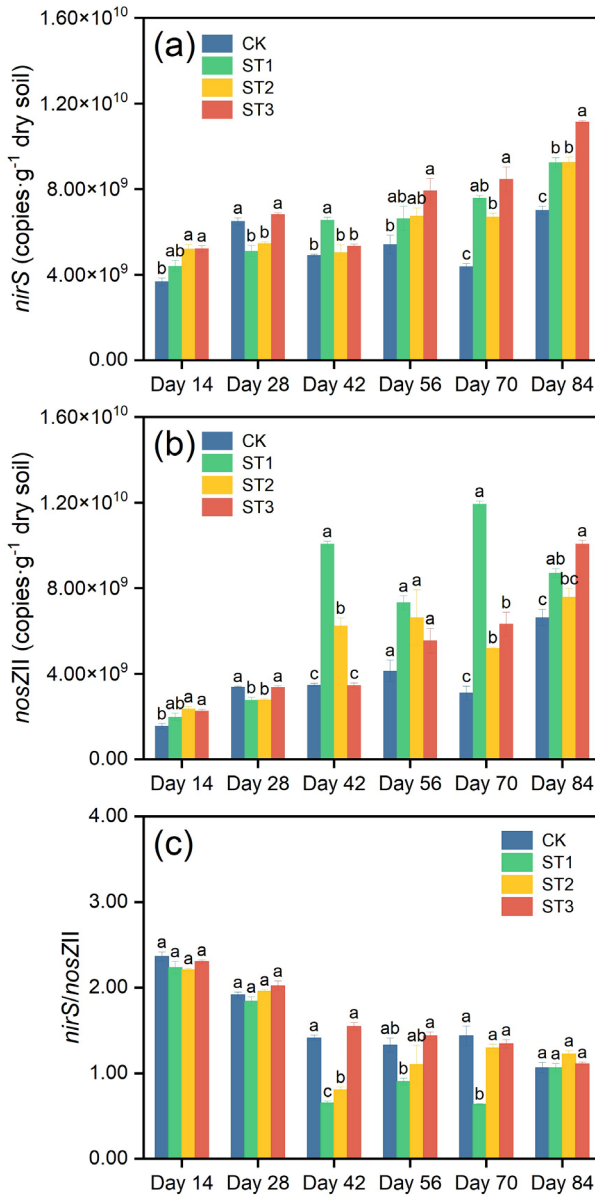
245 **3.4.3 The abundance of N₂O-producing (*nirS*) and N₂O-reducing (*nosZII*) communities**

246 The population size of *nirS* was relatively stable, and the variations among the treatments were negligible under flooding

247 (Fig.5a). However, under drying, the copy number of *nirS* increased and was clearly affected by the straw incorporations. All



248 the straw-amended treatments outstandingly increased *nirS* abundance compared to CK. Among the treatments, ST3
249 possessed the highest copy number of *nirS*, while ST2 and ST1 had similar lower abundances.



250
251 **Figure 5: Dynamics of *nirS* abundance (a), *nosZII* abundance (b), and *nirS/nosZII* ratio (c) during the incubation.**
252 Different lower-case letters denote significant differences between treatments ($\alpha = 0.05$). Data are given in average \pm
253 standard error ($n = 3$).

254 In general, the dynamics of *nosZII* abundance during the incubation were similar to the variations of *nirS* abundance (Fig.5b).
255 Interestingly, the abundance of *nosZII* in ST1 was the highest, which was significantly higher than the second highest
256 treatment (ST3) during drying, especially during the peaking time of N₂O flux on day 70.



257 When concerning the abundance ratio of *nirS/nosZII*, ST1 displayed the lowest average ratio of 0.81, while the average
258 ratios of other treatments were higher, ranging from 1.11 to 1.36 (Fig.5c).

259 **4 Discussion**

260 Rice straw is an important organic resource and has been used to improve soil productivity (Huo et al., 2024; Zhou et al.,
261 2024), which was also observed in this study. Since rice straw return may also exacerbate GHG emissions from paddy fields
262 (Shi et al., 2023; He et al., 2024), which could offset the benefits of rice straw returning to paddy systems, it is urgent to
263 investigate the feasibility of straw incorporation in relation to soil fertility improvement and GHG emission control. We
264 hypothesized that there should be a suitable straw incorporation amount, which could not only modify soil fertility, but also
265 generate minimal GHG emissions without causing a significant increase in GWP.

266 We found that ST1 treatment clearly improved soil physicochemical properties. More importantly, it failed to significantly
267 increase GWP compared to the treatment without straw input (CK). Among CO₂, CH₄, and N₂O, N₂O has the highest
268 warming potential over a 100-year horizon, followed by CH₄ and CO₂ (Forster et al., 2021). It was detected that there were
269 two peaks of N₂O fluxes, which were consistent with other studies (Zhou et al., 2020; Senbayram et al., 2022; Li et al.,
270 2025b): one was under flooding just after nitrogen fertilization and the other occurred during drying. We found that only CK
271 emitted a large amount of N₂O while the emissions from straw-amended treatments were negligible during the flooding
272 phase. This would be partially due to the competition of soil microorganisms for soil available nitrogen. Generally, organic
273 materials incorporated into paddy soil will stimulate mass propagation of soil microorganisms, and these fast reproducing
274 microbial communities will compete for soil free nitrogen as their nutrient (L'espérance et al., 2024; Zhang et al., 2025). On
275 the contrary, the nitrogen fertilizer in CK could be an available nitrogen source for nitrification and denitrification. As a
276 consequence, this treatment emitted a lot of N₂O. However, during drying, oxygen continuously penetrated the soil profile,
277 and abundant available nitrogen was released mainly through the mineralization of soil organic matter. Organic matter also
278 contributed more electron donors to denitrification when the soil moisture declined (Yi et al., 2022). These means if a soil
279 contains higher SOC, it would produce more mineral nitrogen as the substrate and provide more electron donors for N₂O
280 production and reduction. Although ST1 contained slightly higher SOC than CK, there was no clear difference in N₂O fluxes
281 between them during the drying process. The reasons for this phenomenon would be as follows. N₂O emission largely relies
282 on N₂O production ability and consumption activity, which are driven by the related functional microorganisms (Hu et al.,
283 2015). Among these microorganisms, the denitrifiers of *nirS*-type and *nosZII*-type communities were indicated as the active
284 microbial groups in paddy soils (Jones et al., 2013; Wei et al., 2015; Jin et al., 2020; Chen et al., 2024; Yang et al., 2024). It
285 was detected that ST1 treatment contained a relatively low abundance of *nirS* and the highest *nosZII* copy number among the
286 treatments, as well as the lowest *nirS/nosZII* ratio. These results strongly suggested that ST1 would possess relatively low
287 N₂O production and high N₂O transformation capabilities. As a result, the N₂O emission from ST1 was significantly lower
288 than that from CK.



289 Applying organic materials to paddy fields often intensified CH₄ flux from soils (Han et al., 2023; Song et al., 2024; Qin et
290 al., 2025). Similar results were also observed in this study, and the CH₄ emission was significantly and positively related to
291 the straw input rate. Interestingly, the cumulative CH₄ emission from ST1 treatment was quite low with less than 5 g·m⁻².
292 Further increasing the straw incorporation rate sharply elevated CH₄ emission, such as the cumulative CH₄ emissions of ST2
293 and ST3 were about 5 and 9 times those of ST1, respectively. The question is why ST1 treatment maintained such a low
294 level of CH₄ flux. CH₄ emission depends on CH₄ production and consumption in soil, which are driven by methanogens and
295 methanotrophs (Conrad, 2020; Nwokolo and Enebe, 2025). The population size of *mcrA* in ST1 was clearly higher than that
296 in CK but significantly lower than ST2 and ST3, indicating that the CH₄ production capacity of ST1 would be higher than
297 that of CK but lower than the treatments receiving higher amounts of straw. Another important aspect in determining CH₄
298 flux is the soil CH₄ consumption capability (Conrad, 2020; Nwokolo and Enebe, 2025). CH₄ consumption in a soil would be
299 strongly linked to its CH₄ holding capacity (Ariani et al., 2022) because this gas remaining in the soil would be mostly
300 transformed by methanotrophs. Once CH₄ producing ability is over the soil CH₄ holding capacity, the extra CH₄ would be
301 emitted into the atmosphere. We observed that the soil CH₄ holding capacity was about 190 mmol·mol⁻¹ under the anaerobic
302 environment, which was determined from the soil CH₄ concentrations where CH₄ emissions were almost undetectable. We
303 also observed that soil CH₄ concentrations of ST1 fluctuated about 200 mmol·mol⁻¹ under anaerobic conditions, and
304 coincidentally, the CH₄ emission of this treatment was minimal. While the CH₄ concentrations in ST2 and ST3 were clearly
305 over 190 mmol·mol⁻¹, CH₄ emissions notably occurred. Therefore, the CH₄ production activity in ST1 treatment was slightly
306 over the soil CH₄ holding capacity, which would be the main mechanism for its minimal CH₄ flux among straw-amended
307 treatments.

308 5 Conclusion

309 Rice straw could be incorporated into paddy soil at a suitable amount. Compared to no straw input, it could not only improve
310 soil fertility, but also avoid significantly increasing GWP. The major contributors to this consequence were strongly linked
311 to the highest *nosZII* copy number and the lowest *nirS/nosZII* ratio, and the CH₄ producing ability fluctuated around the soil
312 CH₄ holding capacity and most of the produced CH₄ was consumed by soil methanotrophs. Because different soils possess
313 various soil properties, their CH₄ holding capacities and nitrogen transformation processes would be different. Therefore, the
314 feasibilities of straw returning for different soils require further investigations.

315 Data availability

316 Data will be made available on reasonable request.



317 **Supplement link**

318 The link to the supplement will be included by Copernicus, if applicable.

319 **Author contributions**

320 **MZ**: Conceptualization, Data Curation, Formal analysis, Investigation, Methodology, Validation, Visualization, Writing -
321 Original Draft, Writing - Review & Editing. **RL**: Data Curation, Formal analysis. **WZ**: Conceptualization, Resources,
322 Supervision, Writing - Review & Editing. **CF**: Resources. **SGC** and **AT**: Writing - Review & Editing. **BZ**:
323 Conceptualization, Resources, Supervision, Writing - Review & Editing. **WW**: Conceptualization, Methodology, Resources,
324 Supervision, Validation, Writing - Original Draft, Writing - Review & Editing. **RS**: Conceptualization, Funding acquisition,
325 Resources, Supervision, Writing - Original Draft, Writing - Review & Editing.

326 **Competing interests**

327 The authors declare that they have no conflict of interest.

328 **Disclaimer**

329 Publisher's note: Copernicus Publications remains neutral with regard to jurisdictional claims made in the text, published
330 maps, institutional affiliations, or any other geographical representation in this paper. While Copernicus Publications makes
331 every effort to include appropriate place names, the final responsibility lies with the authors. Views expressed in the text are
332 those of the authors and do not necessarily reflect the views of the publisher.

333 **Acknowledgements**

334 We thank Xingan Fu and Xiaohua Yang from Taoyuan Agroecosystem Research Station for their help in soil and gas
335 sampling. We thank Laurent Philippot from INRAE, France for his constructive suggestions in paper writing.

336 **Financial support**

337 This work was supported by the International Partnership Program of Chinese Academy of Sciences (Grant No.
338 092GJHZ2022057FN), and the Training Program for Outstanding Youth of Changsha (Grant No. kq2306030). Simon
339 Guerrero-Cruz received support from the NXPO Thailand under PMU-B, through the European and SE Asia joint funding
340 scheme (JFS-2021-100: Micro-GRICE).



341 **Review statement**

342 The review statement will be added by Copernicus Publications listing the handling editor as well as all contributing referees
343 according to their status anonymous or identified.

344 **References**

345 Ariani, M., Hanudin, E., and Haryono, E.: The effect of contrasting soil textures on the efficiency of alternate wetting-drying
346 to reduce water use and global warming potential, *Agric. Water Manage.*, 274, 107970,
347 <https://doi.org/10.1016/j.agwat.2022.107970>, 2022.

348 Bao, S.: *Soil and Agricultural Chemistry Analysis*, Beijing, China, 2000.

349 Cai, Y., Liu, Z., Zhang, S., Liu, H., Nicol, G. W., and Chen, Z.: Microbial community structure is stratified at the millimeter-
350 scale across the soil–water interface, *ISME Commun.*, 2, 53, <https://doi.org/10.1038/s43705-022-00138-z>, 2022.

351 Cai, Y., Zhang, H., Hu, X., Yang, Y., Hazard, C., Nicol, G. W., He, J., Shen, J., He, Z., Zhang, L., Zhang, J., Liu, H., Zhang,
352 S., and Chen, Z.: Millimeter-scale niche differentiation of N-cycling microorganisms across the soil–water interface has
353 implications for N₂O emissions from wetlands, *ISME J.*, 19, <https://doi.org/10.1093/ismej/owaf062>, 2025.

354 Chen, D., Wang, C., Shen, J., Li, Y., and Wu, J.: Response of CH₄ emissions to straw and biochar applications in double-rice
355 cropping systems: Insights from observations and modeling, *Environ. Pollut.*, 235, 95-103,
356 <https://doi.org/10.1016/j.envpol.2017.12.041>, 2018.

357 Chen, K., Feng, J., Bodelier, P. L. E., Yang, Z., Huang, Q., Delgado-Baquerizo, M., Cai, P., Tan, W., and Liu, Y.: Metabolic
358 coupling between soil aerobic methanotrophs and denitrifiers in rice paddy fields, *Nat. Commun.*, 15, 3471,
359 <https://doi.org/10.1038/s41467-024-47827-y>, 2024.

360 Chen, P., Xu, J., Wang, K., Zhang, Z., Zhou, Z., Li, Y., Li, T., Nie, T., Wei, Q., and Liao, L.: Straw return combined with
361 water-saving irrigation increases microbial necromass accumulation by accelerating microbial growth-turnover in Mollisols
362 of paddy fields, *Geoderma*, 454, 117211, <https://doi.org/10.1016/j.geoderma.2025.117211>, 2025.

363 Chen, Z., Luo, X., Hu, R., Wu, M., Wu, J., and Wei, W.: Impact of long-term fertilization on the composition of denitrifier
364 communities based on nitrite reductase analyses in a paddy soil, *Microb. Ecol.*, 60, 850-861, <https://doi.org/10.1007/s00248-010-9700-z>, 2010.

366 Conrad, R.: Methane production in soil environments—Anaerobic biogeochemistry and microbial life between flooding and
367 desiccation, *Microorganisms*, 8, 881, <https://doi.org/10.3390/microorganisms8060881>, 2020.

368 FAO: FAOSTAT Database, 2020.

369 Forster, P., Storelvmo, T., Armour, K., Collins, W., Dufresne, J.-L., Frame, D., Lunt, D., Mauritsen, T., Palmer, M.,
370 Watanabe, M., Wild, M., and Zhang, H.: Chapter 7: The Earth’s Energy Budget, Climate Feedbacks, and Climate Sensitivity.
371 *Climate Change 2021: The Physical Science Basis. Contribution of Working Group I to the Sixth Assessment Report of the*
372 *Intergovernmental Panel on Climate Change*, UK, USA, 2021.



373 Hallin, S., Philippot, L., Löffler, F. E., Sanford, R. A., and Jones, C. M.: Genomics and ecology of novel N₂O-reducing
374 microorganisms, *Trends Microbiol.*, 26, 43-55, <https://doi.org/10.1016/j.tim.2017.07.003>, 2018.

375 Han, Y., Zhang, Z., Li, T., Chen, P., Nie, T., Zhang, Z., and Du, S.: Straw return alleviates the greenhouse effect of paddy
376 fields by increasing soil organic carbon sequestration under water-saving irrigation, *Agric. Water Manage.*, 287, 108434,
377 <https://doi.org/10.1016/j.agwat.2023.108434>, 2023.

378 Harun, S. N., Hanafiah, M. M., and Noor, N. M.: Rice straw utilisation for bioenergy production: A brief overview, *Energies*,
379 15, 5542, <https://doi.org/10.3390/en1515542>, 2022.

380 He, Z., Cao, H., Qi, C., Hu, Q., Liang, J., and Li, Z.: Straw management in paddy fields can reduce greenhouse gas
381 emissions: A global meta-analysis, *Field Crops Res.*, 306, 109218, <https://doi.org/10.1016/j.fcr.2023.109218>, 2024.

382 Hu, H., Chen, D., and He, J.: Microbial regulation of terrestrial nitrous oxide formation: understanding the biological
383 pathways for prediction of emission rates, *FEMS Microbiol. Rev.*, 39, 729-749, <https://doi.org/10.1093/femsre/fuv021>, 2015.

384 Huo, R., Wang, J., Wang, K., Zhang, Y., Ren, T., Li, X., Cong, R., and Lu, J.: Long-term straw return enhanced crop yield by
385 improving ecosystem multifunctionality and soil quality under triple rotation system: An evidence from a 15 years study,
386 *Field Crops Res.*, 312, 109395, <https://doi.org/10.1016/j.fcr.2024.109395>, 2024.

387 Jiang, Y., Qian, H., Huang, S., Zhang, X., Wang, L., Zhang, L., Shen, M., Xiao, X., Chen, F., Zhang, H., Lu, C., Li, C.,
388 Zhang, J., Deng, A., van Groenigen, K. J., and Zhang, W.: Acclimation of methane emissions from rice paddy fields to straw
389 addition, *Sci. Adv.*, 5, eaau9038, <https://doi.org/10.1126/sciadv.aau9038>, 2019.

390 Jin, W., Cao, W., Liang, F., Wen, Y., Wang, F., Dong, Z., and Song, H.: Water management impact on denitrifier community
391 and denitrification activity in a paddy soil at different growth stages of rice, *Agric. Water Manage.*, 241, 106354,
392 <https://doi.org/10.1016/j.agwat.2020.106354>, 2020.

393 Jones, C. M., Graf, D. R. H., Bru, D., Philippot, L., and Hallin, S.: The unaccounted yet abundant nitrous oxide-reducing
394 microbial community: a potential nitrous oxide sink, *ISME J.*, 7, 417-426, <https://doi.org/10.1038/ismej.2012.125>, 2013.

395 Kong, D., Zhang, X., Yu, Q., Jin, Y., Jiang, P., Wu, S., Liu, S., and Zou, J.: Mitigation of N₂O emissions in water-saving
396 paddy fields: Evaluating organic fertilizer substitution and microbial mechanisms, *J. Integr. Agric.*, 23, 3159-3173,
397 <https://doi.org/10.1016/j.jia.2024.03.047>, 2024.

398 L'Espérance, E., Bouyoucef, L. S., Dozois, J. A., and Yergeau, E.: Tipping the plant-microbe competition for nitrogen in
399 agricultural soils, *iScience*, 27, 110973, <https://doi.org/10.1016/j.isci.2024.110973>, 2024.

400 Lee, J. H., Lee, J. G., Jeong, S. T., Gwon, H. S., Kim, P. J., and Kim, G. W.: Straw recycling in rice paddy: Trade-off between
401 greenhouse gas emission and soil carbon stock increase, *Soil Till. Res.*, 199, 104598,
402 <https://doi.org/10.1016/j.still.2020.104598>, 2020.

403 Li, R., Tian, Y., Wang, F., Sun, Y., Lin, B., Dang, Y. P., Zhao, X., Zhang, H., and Xu, Z.: Optimizing the rate of straw
404 returning to balance trade-offs between carbon emission budget and rice yield in China, *Sustain. Prod. Consump.*, 47, 166-
405 177, <https://doi.org/10.1016/j.spc.2024.03.026>, 2024.

406 Li, S., Nie, J., Liang, H., Zhou, G., Zhang, J., Liao, Y., Lu, Y., Tao, Y., Gao, S., and Cao, W.: Paddy fields can gain high



407 productivity with low net global warming potential by utilizing green manure, *J. Environ. Manage.*, 377, 124596,
408 https://doi.org/10.1016/j.jenvman.2025.124596, 2025a.

409 Li, X., Wang, R., Du, Y., Han, H., Guo, S., Song, X., and Ju, X.: Significant increases in nitrous oxide emissions under
410 simulated extreme rainfall events and straw amendments from agricultural soil, *Soil Till. Res.*, 246, 106361,
411 https://doi.org/10.1016/j.still.2024.106361, 2025b.

412 Liu, C., Zhang, W., Hou, H., Liao, R., Wei, W., and Sheng, R.: Effect of long-term land use on the *nosZI*- and *nosZII*-
413 containing microbial communities, *Appl. Soil Ecol.*, 189, 104961, https://doi.org/10.1016/j.apsoil.2023.104961, 2023a.

414 Liu, H., Sun, L., Zhou, G., Wan, L., Li, G., Chen, X., Qin, W., Lin, Y., and Liu, J.: Delayed flooding after green manure
415 incorporation decreases methane emissions and greenhouse gas intensity in rice paddy fields, *Geoderma*, 462, 117528,
416 https://doi.org/10.1016/j.geoderma.2025.117528, 2025.

417 Liu, L., Liu, D., Ding, X., Chen, M., and Zhang, S.: Straw incorporation and nitrogen fertilization enhance soil carbon
418 sequestration by altering soil aggregate and microbial community composition in saline-alkali soil, *Plant Soil*, 341-356
419 https://doi.org/10.1007/s11104-023-06439-z, 2023b.

420 Nan, Q., Fang, C., Cheng, L., Hao, W., and Wu, W.: Elevation of NO_3^- -N from biochar amendment facilitates mitigating
421 paddy CH_4 emission stably over seven years, *Environ. Pollut.*, 295, 118707, https://doi.org/10.1016/j.envpol.2021.118707,
422 2022.

423 Nwokolo, N. L. and Enebe, M. C.: Methane production and oxidation—A review on the *pmoA* and *mcrA* gene abundances for
424 understanding the functional potentials of agricultural soils, *Pedosphere*, 35, 161-181,
425 https://doi.org/10.1016/j.pedsph.2024.05.006, 2025.

426 Qin, J., Long, X., Zhou, Y., Jiang, L., and Yuan, P.: Straw incorporation mitigates methane emissions by facilitating the
427 conversion of particulate organic carbon to mineral-associated organic carbon, *Agric. Ecosyst. Environ.*, 393, 109780,
428 https://doi.org/10.1016/j.agee.2025.109780, 2025.

429 Qin, X., Lu, Y., Wan, Y., Wang, B., Nie, J., Li, Y. e., and Liao, Y.: Rice straw application improves yield marginally and
430 increases carbon footprint of double cropping paddy rice (*Oryza sativa* L.), *Field Crops Res.*, 291, 108796,
431 https://doi.org/10.1016/j.fcr.2022.108796, 2023.

432 Senbayram, M., Wei, Z., Wu, D., Shan, J., Yan, X., and Well, R.: Inhibitory effect of high nitrate on N_2O reduction is offset
433 by long moist spells in heavily N loaded arable soils, *Biol. Fertil. Soils*, 58, 77-90, https://doi.org/10.1007/s00374-021-
434 01612-x, 2022.

435 Shen, J., Tang, H., Liu, J., Wang, C., Li, Y., Ge, T., Jones, D. L., and Wu, J.: Contrasting effects of straw and straw-derived
436 biochar amendments on greenhouse gas emissions within double rice cropping systems, *Agric. Ecosyst. Environ.*, 188, 264-
437 274, https://doi.org/10.1016/j.agee.2014.03.002, 2014.

438 Shi, W., Fang, Y., Chang, Y., and Xie, G.: Toward sustainable utilization of crop straw: Greenhouse gas emissions and their
439 reduction potential from 1950 to 2021 in China, *Resour. Conserv. Recycl.*, 190, 106824,
440 https://doi.org/10.1016/j.resconrec.2022.106824, 2023.



441 Song, H. J., Park, S. Y., Chae, H. G., Kim, P. J., and Lee, J. G.: Benefits of organic amendments on soil C stock may be offset
442 by increased methane flux in rice paddy field, *Agric. Ecosyst. Environ.*, 359, 108742,
443 https://doi.org/10.1016/j.agee.2023.108742, 2024.

444 Van Hung, N., Maguyon-Detras, M. C., Migo, M. V., Quilloy, R., Balingbing, C., Chivenge, P., and Gummert, M.: Rice
445 straw overview: Availability, properties, and management practices, in: Sustainable Rice Straw Management, edited by:
446 Gummert, M., Hung, N. V., Chivenge, P., and Douthwaite, B., Springer International Publishing, Cham, 1-13,
447 https://doi.org/10.1007/978-3-030-32373-8_1, 2020.

448 Wang, L., Sheng, R., Yang, H., Wang, Q., Zhang, W., Hou, H., Wu, J., and Wei, W.: Stimulatory effect of exogenous nitrate
449 on soil denitrifiers and denitrifying activities in submerged paddy soil, *Geoderma*, 286, 64-72,
450 https://doi.org/10.1016/j.geoderma.2016.10.023, 2017.

451 Wang, W., Lai, D. Y. F., Sardans, J., Wang, C., Datta, A., Pan, T., Zeng, C., Bartrons, M., and Peñuelas, J.: Rice straw
452 incorporation affects global warming potential differently in early vs. late cropping seasons in Southeastern China, *Field
453 Crops Res.*, 181, 42-51, https://doi.org/10.1016/j.fcr.2015.07.007, 2015.

454 Wang, X., Yang, Z., Liu, X., Huang, G., Xiao, W., and Han, L.: The composition characteristics of different crop straw types
455 and their multivariate analysis and comparison, *Waste Manage.*, 110, 87-97, https://doi.org/10.1016/j.wasman.2020.05.018,
456 2020.

457 Wei, W., Isobe, K., Nishizawa, T., Zhu, L., Shiratori, Y., Ohte, N., Koba, K., Otsuka, S., and Senoo, K.: Higher diversity and
458 abundance of denitrifying microorganisms in environments than considered previously, *ISME J.*, 9, 1954-1965,
459 https://doi.org/10.1038/ismej.2015.9, 2015.

460 Yang, L., Li, S., Shangguan, H., Qiao, Z., Huang, X., Zhou, S., Li, H., Su, X., Sun, X., Zhu, Y., and Yang, X.: Diversity and
461 activity of soil N₂O-reducing bacteria shaped by urbanization, *Environ. Sci. Technol.*, 58, 17295-17303,
462 https://doi.org/10.1021/acs.est.4c01750, 2024.

463 Yi, L., Sheng, R., Wei, W., Zhu, B., and Zhang, W.: Differential contributions of electron donors to denitrification in the
464 flooding-drying process of a paddy soil, *Appl. Soil Ecol.*, 177, 104527, https://doi.org/10.1016/j.apsoil.2022.104527, 2022.

465 Yin, H., Zhao, W., Li, T., Cheng, X., and Liu, Q.: Balancing straw returning and chemical fertilizers in China: Role of straw
466 nutrient resources, *Renew. Sust. Energ. Rev.*, 81, 2695-2702, https://doi.org/10.1016/j.rser.2017.06.076, 2018.

467 Yuan, S., Linquist, B. A., Wilson, L. T., Cassman, K. G., Stuart, A. M., Pede, V., Miro, B., Saito, K., Agustiani, N., Aristya,
468 V. E., Krisnadi, L. Y., Zanon, A. J., Heinemann, A. B., Carracelas, G., Subash, N., Brahmanand, P. S., Li, T., Peng, S., and
469 Grassini, P.: Sustainable intensification for a larger global rice bowl, *Nat. Commun.*, 12, 7163,
470 https://doi.org/10.1038/s41467-021-27424-z, 2021.

471 Zhang, N., Bai, L., Wei, X., Li, T., Tang, Y., Wen, J., Peng, Z., Zhang, Y., Wang, Y., Zeng, X., and Su, S.: Effects of organic
472 material addition on carbon cycling and soil fertility in paddy soil, *J. Environ. Manage.*, 379, 124898,
473 https://doi.org/10.1016/j.jenvman.2025.124898, 2025.

474 Zhou, J., Tang, S., Pan, W., Liu, X., Han, K., Si, L., Ma, Q., Mao, X., Fu, H., and Wu, L.: Long-term non-flooded cultivation



475 with straw return maintains rice yield by increasing soil pH and soil quality in acidic soil, Eur. J. Agron., 159, 127208,
476 <https://doi.org/10.1016/j.eja.2024.127208>, 2024.
477 Zhou, W., Jones, D. L., Hu, R., Clark, I. M., and Chadwick, D. R.: Crop residue carbon-to-nitrogen ratio regulates denitrifier
478 N₂O production post flooding, Biol. Fertil. Soils, 56, 825-838, <https://doi.org/10.1007/s00374-020-01462-z>, 2020.